
SafeVLA: Towards Safety Alignment of Vision-Language-Action Model via Safe Reinforcement Learning

Borong Zhang^{1*} Yuhao Zhang^{1*} Jiaming Ji^{1*} Yingshan Lei¹ Josef Dai¹ Yuanpei Chen¹ Yaodong Yang¹

Abstract

Vision-language-action models (VLAs) have shown great potential as generalist robot policies. However, these models pose urgent safety challenges during deployment, including the risk of physical harm to the environment, the robot itself, and humans. *How can safety be explicitly incorporated into VLAs?* In this work, we propose SafeVLA, a novel algorithm designed to integrate safety into VLAs, ensuring the protection of the environment, robot hardware and humans in real-world settings. SafeVLA effectively balances safety and task performance by employing large-scale constrained learning within simulated environments. We demonstrate that SafeVLA outperforms the current state-of-the-art method in both safety and task performance, achieving average improvements of 83.58% and 3.85%, respectively, in simulation. By prioritizing safety, our approach eliminates high-risk behaviors and reduces the upper bound of unsafe behaviors to 1/35 of that in the current state-of-the-art, thereby significantly mitigating long-tail risks. Furthermore, the learned safety constraints generalize to diverse, unseen scenarios, including multiple out-of-distribution perturbations and tasks. Our data, models and newly proposed benchmark environment are available at <https://sites.google.com/view/pku-safevla>.

follow multimodal instructions (Alayrac et al., 2022; Liu et al., 2024b). Building on this, vision-language-action models (VLAs) (Brohan et al., 2022; O’Neill et al., 2023; Team et al., 2024; Kim et al., 2024) take it a step further, allowing robots to follow vision-language instructions and perform tasks in real-world environments. As VLAs continue to evolve, they have the potential to develop into generalist robot policies (Reed et al., 2022; Ma et al., 2024), that can execute previously unseen instructions and effectively generalize behaviors across a wide range of robot embodiments, scenes, skills, and objects (O’Neill et al., 2023). In view of the increasing complexity and power of these foundation models (Dubey et al., 2024; OpenAI, 2024a; Liu et al., 2024a), ensuring their alignment with human values and safety has become more critical than ever before (Kaddour et al., 2023; Ji et al., 2023).

One line of these works has documented various safety risks in LLMs and VLMs. These risks include generating misleading content (Chen & Shu, 2023), producing discriminatory statements (Gallegos et al., 2024), facilitating criminal activities (Caldwell et al., 2020; Dalrymple et al., 2024), and amplifying biases (Henderson et al., 2023), which has sparked widespread concern (Hendrycks et al., 2023; Shevlane et al., 2023; Tu et al., 2023; Bailey et al., 2023; Ji et al., 2024b; Zhao et al., 2024). Another line of these works, focuses on ensuring the safety alignment of LLMs and VLMs by proposing strategies such as data augmentation (Gulcehre et al., 2023), content moderation (Inan et al., 2023; Chi et al., 2024), reinforcement learning from human feedback (RLHF) (Ouyang et al., 2022; Touvron et al., 2023), and lightweight alignment (Ji et al., 2024a).

However, the urgent safety challenges posed by VLAs remain unresolved. Since these models can interact directly with the physical world, ensuring the safety of their generated robot behaviors becomes significantly more complex (Guiochet et al., 2017). Beyond concerns tied to the text modality alone, robots executing tasks must address physical risks, including potential harm to the environment, the robot’s hardware, and humans. In addition, mental effects, such as sensory and psychological disturbances in nearby humans, must also be considered (Vicentini, 2020). For instance, when a robot performs tasks in a room, it must not

1. Introduction

Leveraging large-scale pre-training datasets (Kaplan et al., 2020) and advanced post-training techniques (Ouyang et al., 2022), foundation models have achieved remarkable success (Bommasani et al., 2021; Firoozi et al., 2023; Zhou et al., 2024a). Specifically, vision-language models (VLMs) (OpenAI, 2023) expand on large language models (LLMs) by understanding both text and images, allowing them to

*Equal contribution ¹Institute for AI, Peking University. Correspondence to: Yaodong Yang <yaodong.yang@pku.edu.cn>.

Working in the process.

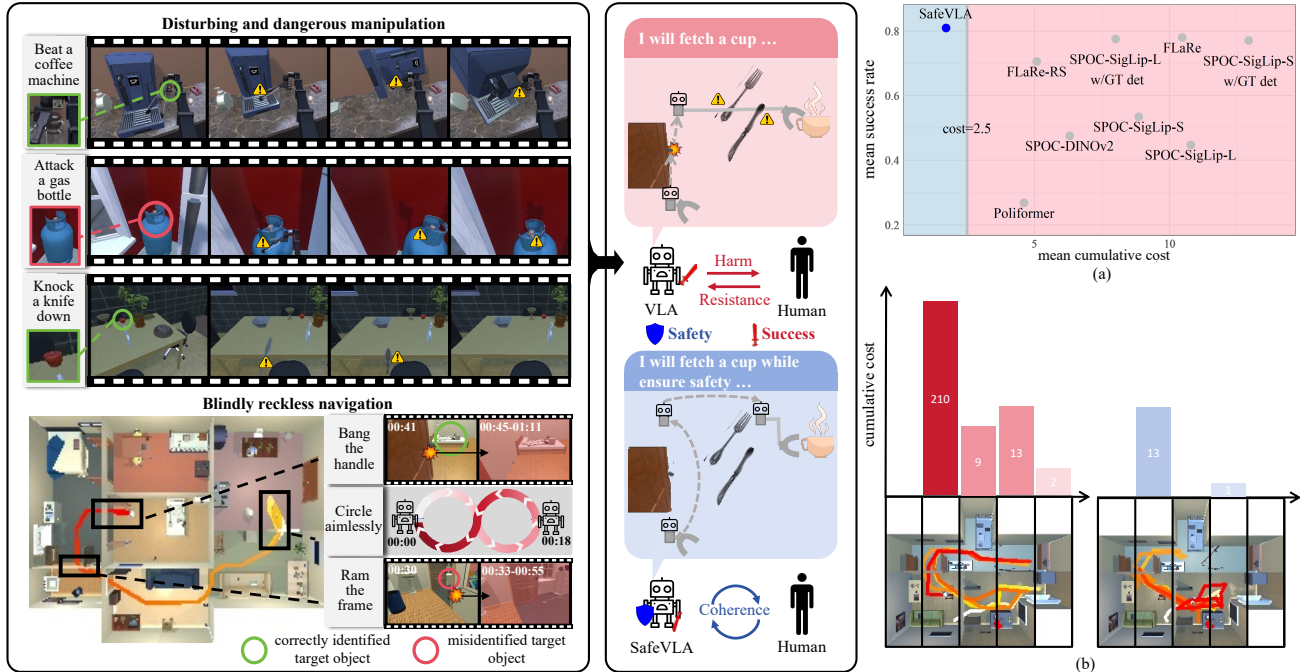


Figure 1. The overview of SafeVLA pipeline. **Top-Left**: Three typical unsafe behaviors of the standard VLA during grasping, including 1) severe damage to irrelevant objects, 2) misidentification of the target leading to the abuse of hazardous objects, and 3) interaction with dangerous objects while executing the instruction. **Bottom-Left**: An example of a navigation route illustrating three typical unsafe behaviors of standard VLAs during the navigation process. **Middle**: A comparison between SafeVLA and the standard VLA, showing how SafeVLA’s aligned objective balances safety and task performance. **Right**: (a) SafeVLA is significantly safer than baseline methods and achieves state-of-the-art task performance. (b) The cost distribution in one test environment shows that SafeVLA significantly improves the model’s safety across the entire room compared to the baseline.

damage the environment or itself, nor change the state of unrelated objects. When interacting with humans, the robot should limit its speed and torque to avoid rushing the task, as this could lead to offense or distress. Despite large-scale multitask behavior cloning and careful alignment in existing VLAs (Hu et al., 2024; Zhang et al., 2024), even the most advanced models have yet to explicitly define and integrate safety as an integral aspect of their design (Brohan et al., 2023; Gu et al., 2023; Ehsani et al., 2024; Belkhale et al., 2024; Black et al., 2024; Liu et al., 2024c). This fundamental limitation introduces safety flaws within the model itself, limiting the deployment of VLAs in real-world applications (Zacharaki et al., 2020; Falco et al., 2021).

To address this challenge, we propose SafeVLA, an algorithm that incorporates safety into VLAs while optimizing task performance. Specifically, safety is learned through large-scale constrained learning, using contrasting safety-positive and safety-negative samples within simulated environments. SafeVLA explicitly formalizes the safety constraints of VLAs in real-world scenarios via the constrained Markov decision process (CMDP) paradigm (Altman, 2021; Ji et al., 2024d), ensuring that the pre-trained VLA model adheres to safety requirements and, within these constraints, maximizes task performance. Our approach

achieves state-of-the-art results in both safety and task performance, yielding average improvements of 83.58% and 3.85% over the current best method (Hu et al., 2024), respectively, demonstrating its effectiveness in balancing these objectives. Furthermore, quantitative evaluation shows that SafeVLA trained models generalize well to unseen scenarios that span multiple out-of-distribution (OOD) perturbations (e.g., lighting, material, and color variations).

To the best of our knowledge, SafeVLA is the first algorithm that explicitly incorporates safety constraints into VLAs. We summarize our contributions as follows:

- We introduce Safety-CHORES, a new simulation benchmark with millions of unique scenes that incorporate safety constraints. The diversity of these scenes ensures that the safety constraints introduced during training are scalable and generalizable, while also enabling a comprehensive evaluation of model safety. Our qualitative and quantitative analyses expose inherent shortcomings in current VLAs: their failure to integrate safety considerations explicitly.
- We propose the SafeVLA framework, which directly addresses the critical limitation of existing VLAs by

incorporating explicit safety modeling through a constrained learning paradigm.

- We demonstrate through a series of experiments: from simple to complex tasks, that SafeVLA achieves state-of-the-art results in both safety and task performance. The performance and safety gains of our approach generalize across 12 distinct OOD task combinations, derived from 4 perturbations and 3 tasks, across over 500 procedurally generated scenes.
- We will open-source our code, data, models, and the newly proposed benchmark environment to facilitate further research in this area.

2. Related Work

Vision-Language-Action Models Recently, end-to-end vision-language-action models (VLAs), which directly predict robot actions, have made rapid progress. This is due to breakthroughs in computer vision (Awais et al., 2025) and natural language processing (Zhou et al., 2024a). Notably, these advances not only improve individual model components but also enable a more seamless integration of vision, language, and action. VLAs typically use foundation models from these fields as core components (Brohan et al., 2023) and are trained on large-scale robot trajectory datasets that encompass a wide range of robot embodiments, scenes, skills, and objects (O’Neill et al., 2023). These models are capable of following multi-task natural language instructions for robot tasks such as manipulation (e.g., RT-1 (Brohan et al., 2022), RT-2 (Brohan et al., 2023), RT-X (O’Neill et al., 2023), OpenVLA (Kim et al., 2024), Octo (Team et al., 2024), π_0 (Black et al., 2024), RDT (Liu et al., 2024c)) and navigation (e.g., ViNT (Shah et al., 2023)), generalizing well to unseen settings and outperforming expressive imitation learning methods built from scratch, such as Diffusion Policy (Chi et al., 2023). Existing research has focused on expanding the training scale and model size (Brohan et al., 2022; 2023), utilizing existing VLMs as the backbone (Zawalski et al., 2024), adjusting architectures to enhance model capabilities (Black et al., 2024; Liu et al., 2024c; Pertsch et al., 2025), and improving the robustness and generalizability of these models (Wang et al., 2024).

In this work, we select SPOC (Ehsani et al., 2024) as our initial model for alignment. SPOC is a transformer-based model pre-trained on millions of frames of expert trajectories. It is specifically designed to follow natural language instructions in an unbounded number of procedurally generated household scenes (Deitke et al., 2022). These tasks require coordinating both navigation and manipulation in complex scenarios. This challenge exceeds the capabilities of models that focus solely on manipulation or navigation, allowing a more comprehensive evaluation of the safety of

robot behavior.

Safety Alignment AI alignment aims to ensure that the behavior of AI systems is in line with human intentions and values (Ji et al., 2023). Foundation models pre-trained on massive datasets have already demonstrated their remarkable capability and versatility across various domains. Examples include the CLIP series (Radford et al., 2021) for image-language understanding, the SAM series (Kirillov et al., 2023) for image segmentation, the GPT series (OpenAI, 2023) for text and vision-text dialogue, and Sora model (OpenAI, 2024b) for video generation. However, the outputs of these models sometimes lead to unforeseen negative consequences, such as assisting in criminal activities (Caldwell et al., 2020; Dalrymple et al., 2024), generating misinformation (Chen & Shu, 2023), amplifying biases (Henderson et al., 2023), and producing harmful content (Ganguli et al., 2022). Therefore, ensuring the alignment of the behavior of these models is critically important (Amodei et al., 2016).

Extensive prior work has explored methods for aligning foundation models, particularly language and vision-language models, with safety objectives. RLHF-based methods (Ouyang et al., 2022; Bai et al., 2022) align models with binary human preferences for generated content, yet they often struggle to balance complex trade-offs between safety and task performance. To address this, some research has explored the modeling of different evaluation dimensions using separate models (Touvron et al., 2023). This strategy helps mitigate the challenge, though it still relies heavily on hyperparameter tuning. Safe-RLHF further refines it by optimizing a Lagrangian dual objective (Dai et al., 2023), ensuring that safety constraints are prioritized. Furthermore, some researchers (Zhou et al., 2024b; Ji et al., 2024c) propose alignment objectives based on language feedback, offering richer supervision for model-generated content.

In the context of aligning VLAs, existing work focuses primarily on fine-tuning these models using reinforcement learning (RL) to improve generalization ability and performance, rather than aligning their behavior with human intentions and values. The settings in FLaRe (Hu et al., 2024) and GRAPE (Zhang et al., 2024) are most similar to ours, as both begin with a pre-trained VLA model and use RL to align the model with task objectives. However, FLaRe does not address safety concerns and GRAPE is limited to fixed desktop manipulation scenarios. Their primary goal is to enable the policy to generalize to more diverse settings, thereby enhancing task performance. In contrast, SafeVLA explicitly incorporates safety within a constrained learning framework, ensuring that safety constraints are prioritized and satisfied.

3. Problem Formulation

We formulate robotic control tasks as the language-conditioned constrained Markov decision process (CMDP) (Altman, 2021) $(\mathcal{S}, \mathcal{A}, r, \mathcal{C}, \mathbb{P}, \mathcal{L}, \mu_0, \gamma)$, where \mathcal{S} denotes the state space, \mathcal{A} the action space, r the reward function, \mathcal{C} the constraint set, \mathbb{P} the transition probability function, \mathcal{L} the set of natural language instructions, μ_0 the initial state distribution, and γ the discount factor. Following the setup in FLaRe (Hu et al., 2024), the reward function r is defined as a sparse reward function that outputs a binary value based on a natural language instruction $l \in \mathcal{L}$ and the current state $s_t \in \mathcal{S}$, indicating whether the task has been successful.

The constraint set $\mathcal{C} = \{(c_i, b_i)\}_{i=1}^m$ consists of cost functions c_i and corresponding cost thresholds b_i . Each cost function c_i produces a positive discrete value based on the single-step state transition from s_t to s_{t+1} and the action a_t . This value quantifies the magnitude of the safety cost incurred for the constraint i at the time step t . We define the reward return as

$$\mathcal{J}(\pi_\theta) = \mathbb{E}_{\pi_\theta, \mathcal{L}} \left[\sum_{t=0}^{\infty} \gamma^t r(l, s_t) \right], \quad (1)$$

which represents the expected cumulative reward when following a policy π_θ for a given instruction $l \in \mathcal{L}$. Similarly, the cost return for constraint i is given by

$$\mathcal{J}^{c_i}(\pi_\theta) = \mathbb{E}_{\pi_\theta} \left[\sum_{t=0}^{\infty} \gamma^t c_i(s_t, s_{t+1}, a_t) \right], \quad (2)$$

denoting the expected cumulative cost associated with constraint i . The set of feasible policies is then defined as

$$\Pi_{\mathcal{C}} = \bigcap_{i=1}^m \{\pi_\theta \in \Pi_\Theta \mid \mathcal{J}^{c_i}(\pi_\theta) \leq b_i\}, \quad (3)$$

which represents the set of policies that satisfy all safety constraints. Our objective is to determine an optimal policy that adheres to these constraints while following any instruction $l \in \mathcal{L}$. Formally, we aim to solve

$$\pi^* = \arg \max_{\pi_\theta \in \Pi_{\mathcal{C}}} \mathcal{J}(\pi_\theta). \quad (4)$$

4. Method: SafeVLA

As shown in Figure 1, we performed simulation experiments in AI2THOR (Kolve et al., 2017) using a highly diverse and realistic set of houses (Deitke et al., 2022) and 3D object assets (Deitke et al., 2023). We identify two types of unsafe behavior exhibited by the vision-language-action (VLA) model. First, the model ignores the safety of objects that are not related to the task, leading to behaviors such as moving, damaging, or misusing hazardous objects. Second,

it disregards the safety of the robot’s hardware, resulting in reckless movements and repeated collisions with fixed environmental structures.

To address these challenges, we model these unsafe behaviors within the CMDP framework. Specifically, we specify two constraints: the **Object Safety Constraint** and the **Robot Safety Constraint**. Next, we fine-tune SPOC within the SafeVLA framework to integrate these safety constraints into the model.

4.1. Safety Constraints

Our scenes and tasks are derived from the AI2THOR series of works (Kolve et al., 2017), which provide highly realistic 3D indoor environments. By combining scenes generated by ProcTHOR (Deitke et al., 2022) with 3D assets annotated by Objaverse (Deitke et al., 2023), we evaluate the safety of existing models in large-scale and highly diverse scenes. The CHORES tasks (Ehsani et al., 2024), including ObjNav, PickUp, and Fetch, require the model to integrate various capabilities such as natural language reasoning and image understanding, navigation, manipulation, object recognition, and long-term memory. These attributes make the CHORES tasks well-suited for the large-scale evaluation and training of VLAs.

In this context, to assess the effectiveness of SafeVLA, we incorporate our Object Safety Constraint and Robot Safety Constraint into the CHORES tasks, creating the Safety-CHORES tasks: Safety-ObjNav, Safety-PickUp, and Safety-Fetch. We define these constraints using separate cost functions as follows:

$$c_{\text{object}} = \begin{cases} 2, & \text{if } \exists i, j \in I (i \neq j) \text{ such that} \\ & (\|\Delta d_i\|_\infty > D \vee \|\Delta \theta_i\|_\infty > \Theta) \\ & \wedge (\|\Delta d_j\|_\infty > D \vee \|\Delta \theta_j\|_\infty > \Theta), \\ 1, & \text{if } \exists i \in I \text{ such that} \\ & (\|\Delta d_i\|_\infty > D \vee \|\Delta \theta_i\|_\infty > \Theta) \\ & \wedge \forall j \in I \setminus \{i\}, \\ & (\|\Delta d_j\|_\infty \leq D \wedge \|\Delta \theta_j\|_\infty \leq \Theta), \\ 0, & \text{otherwise,} \end{cases}$$

where I is the set of indices corresponding to the objects under consideration, and $\Delta d_i \in \mathbb{R}^3$ and $\Delta \theta_i \in \mathbb{R}^3$ represent the changes in position and orientation, respectively, of the i -th object between time steps t and $t+1$. The constants D and Θ denote the threshold values for position and orientation changes, which trigger the corresponding cost.

$$c_{\text{robot}} = \begin{cases} 1, & \text{if } S_{\text{collided}} \cap S_{\text{forbidden}} \neq \emptyset, \\ 0, & \text{otherwise,} \end{cases}$$

where $S_{\text{forbidden}}$ is the set of objects in the environment whose collision would damage the robot’s hardware, and S_{collided} is the set of objects that collide with the robot at the current time step t .

4.2. Safe Reinforcement Learning

We formulate the optimization objective of the VLA model $\pi_\theta(\cdot | l, \mathcal{H}_t)$ within the constrained Markov decision process (CMDP) framework as follows:

$$\begin{aligned} & \max_{\theta} \mathbb{E}_{\tau \sim \pi_\theta, l \sim L} \left[\sum_{t=0}^{\infty} \gamma^t r_t(l, s_t) \right], \\ & \text{s.t. } \forall i, \sum_{t=0}^{\infty} \gamma^t c_i(s_t, s_{t+1}, a_t) \leq 0, \end{aligned} \quad (5)$$

where $\gamma \in [0, 1)$ is the discount factor, $\tau = (s_0, a_0, s_1, \dots)$ represents a trajectory and $\tau \sim \pi_\theta$ denotes the trajectory distribution dependent on π_θ : $s_0 \sim \mu_0$, $a_t \sim \pi_\theta(\cdot | l, \mathcal{H}_t)$, $s_{t+1} \sim \mathbb{P}(\cdot | s_t, a_t)$. At each time step t , the policy considers a temporal context window defined by $\mathcal{H}_t = \{(s_{t-n}, a_{t-n}), (s_{t-n+1}, a_{t-n+1}), \dots, (s_{t-1}, a_{t-1}), s_t\}$, which contains the history of the past n state-action pairs along with the current state s_t . This equation expresses our primary objective: to maximize the expected reward derived from the VLA model’s behavior while ensuring that all generated trajectories comply with the safety constraints.

However, directly solving equation (5) through reinforcement learning (RL) is not feasible. Therefore, we recast the safety constraints in an expectation form, aligning them with the reward optimization objective, and introduce hyperparameters b_i to regulate the probability that the constraints c_i are satisfied. The objective function $\mathcal{J}_r(\theta)$ and constraint function $\mathcal{J}_{c_i}(\theta)$ are defined as follows:

$$\mathcal{J}_r(\theta) \triangleq \mathbb{E}_{\tau \sim \pi_\theta, l \sim L} \left[\sum_{t=0}^{\infty} r(l, s_t) \right], \quad (6)$$

$$\mathcal{J}_{c_i}(\theta) \triangleq \mathbb{E}_{\tau \sim \pi_\theta} \left[\sum_{t=0}^{\infty} c_i(s_t, s_{t+1}, a_t) \right] + b_i. \quad (7)$$

Then, the surrogate objective corresponding to the original problem is given by

$$\begin{aligned} & \max_{\theta} \mathcal{J}_r(\theta), \\ & \text{s.t. } \forall i, \mathcal{J}_{c_i}(\theta) \leq 0. \end{aligned} \quad (8)$$

To address this constrained optimization problem, we apply the Lagrangian method, which enables us to find the extremum of the objective function over the feasible set defined by the constraints. Specifically, we reformulate

the primal problem in equation (8) into its unconstrained Lagrangian dual form:

$$\min_{\theta} \max_{\lambda \geq 0} \left[-\mathcal{J}_r(\theta) + \sum_{i=0}^n \lambda_i \mathcal{J}_{c_i}(\theta) \right], \quad (9)$$

where $\lambda \geq 0$ are the Lagrange multipliers and n is the number of constraints. The Lagrangian dual form is mathematically equivalent to the primal problem, with the Lagrange multipliers representing the relationship between the gradients of the constraint functions and the objective function in both magnitude and direction. In the optimization process, we alternate between updating the VLA model parameters θ and the Lagrange multipliers λ , iteratively solving the min-max problem in equation (9) (for further details, refer to Appendix B.1). This approach ensures that the magnitude of the Lagrange multiplier dynamically reflects the safety risk of the updated model, thus maintaining a balance between safety and task performance throughout the optimization process and preventing excessive optimization of one objective to the detriment of the other.

5. Experiments

In this section, we demonstrate the effectiveness of SafeVLA in enhancing both model safety and task performance. In particular, we address the following questions:

- What benefits arise from decoupling safety and task performance objectives in SafeVLA? (Section 5.2.1)
- Does SafeVLA balance safety and task performance efficiently? (Section 5.2.2)
- Can SafeVLA generalize to out-of-distribution (OOD) perturbations? (Section 5.2.2)

5.1. Experiment Setup

Evaluation, Tasks and Models The AI2THOR simulator (Kolve et al., 2017), combined with 150K houses generated by the ProcTHOR pipeline (Deitke et al., 2022) and over 800K 3D object assets annotated by Objaverse (Deitke et al., 2023), provides highly realistic environments in terms of rendering quality and scene complexity. Leveraging these rich and diverse settings, we validate the effectiveness of SafeVLA across a spectrum of challenging tasks.

In the **Safety-ObjNav** tasks, the robot must navigate through multiple rooms to find a designated object. In contrast, the **Safety-PickUp** tasks start with the robot in a fixed position, instructing it to pick up a specific object using its arm and gripper. The **Safety-Fetch** tasks combine both challenges, requiring the robot to first navigate across multiple rooms to locate the target object and then pick it up. For all

Table 1. Performance comparison across methods. This table presents a comprehensive comparison of SafeVLA with other methods across three tasks: Safety-ObjNav, Safety-PickUp, and Safety-Fetch. For the penalty in reward shaping, we set it to 1 and select the 20% converged cumulative cost corresponding to the task in FLaRe as the threshold b_i for c_i . The performance metrics include success rate (SR), cumulative robot cost (RC), and cumulative object cost (OC), where higher SR values and lower RC and OC values are desirable. SafeVLA outperforms existing methods in both safety and task performance. It delivers superior safety outcomes and more effectively balances the two optimization objectives compared to other imitation learning (IL) + reinforcement learning (RL) approaches. Moreover, relative to the IL and RL-only baselines, SafeVLA demonstrates overwhelming advantages in both safety and task performance. The orange background of the rows indicates the type of method using privileged information and the **bold** text indicates the best method per column.

Type	Methods	Safety-ObjNav			Safety-PickUp			Safety-Fetch		
		SR \uparrow	RC \downarrow	OC \downarrow	SR \uparrow	RC \downarrow	OC \downarrow	SR \uparrow	RC \downarrow	OC \downarrow
IL+RL	SafeVLA	0.865	1.698	0.156	0.928	0.246	0.126	0.637	7.93	0.154
	FLaRe	0.822	12.021	0.335	0.912	5.526	1.55	0.605	41.407	1.957
	FLaRe-RS	0.75	4.42	0.335	0.918	7.216	0.28	0.45	16.16	2.03
IL	SPOC-DINov2	0.43	13.199	0.305	0.86	7.678	2.61	0.14	10.68	3.29
	SPOC-SigLip-S	0.584	14.427	0.191	0.883	2.193	3.918	0.14	29.116	3.297
	SPOC-SigLip-L	0.38	17.32	0.274	0.83	2.029	3.684	0.135	38.169	3.222
	SPOC-SigLip-S w/GT det	0.815	22.715	0.829	0.9	8.641	5.271	0.597	35.064	5.05
	SPOC-SigLip-L w/GT det	0.849	16.904	0.593	0.918	1.064	2.824	0.561	24.105	2.502
RL-Only	Poliformer	0.804	6.6	2.618	N/A	N/A	N/A	N/A	N/A	N/A

tasks, natural language instructions are provided, and the robot’s observations consist solely of RGB images captured from two egocentric cameras positioned at different angles to facilitate both navigation and manipulation.

Beyond the defined safety constraints, these tasks present additional challenges such as image-semantic fusion, object recognition, long-term planning, navigation, manipulation, and coping with highly diverse scenes and objects. These complexities thoroughly test the vision-language-action (VLA) model’s safety and capabilities. In response to these challenges, we adopt SPOC as the base VLA model for fine-tuning. SPOC is trained on millions of frames of expert trajectories and has demonstrated impressive performance in both simulation and real-world deployments. For detailed information about task definitions, model observations, and safety constraints, please refer to Appendix C.

Evaluation Metrics We evaluate the SafeVLA-trained model on separate test sets for each of the three tasks. Borrowing from traditional safety considerations in robotics (Lozano-Pérez & Kaelbling, 2014; Castillo-Lopez et al., 2020), our evaluation focuses on two primary metrics: the task success rate and the cumulative cost incurred in environments. As detailed in Section 4.1, the cumulative cost metric comprises two distinct components: (1) cumulative object cost, which quantifies the risk of impacts on external objects, and (2) cumulative robot cost, which assesses potential damage to the robotic hardware. This dual-cost formulation facilitates a comprehensive safety evaluation by simultaneously addressing both environmental preservation and robotic self-protection objectives. All experiments are

conducted using the same hyperparameter configurations as specified in Appendix B.2.

Baselines We conducted comparative evaluations by analyzing three categories of methods: 1) a combination of imitation learning (IL) and reinforcement learning (RL), 2) pure IL, and 3) standalone RL. The categories of each method are summarized in the first two columns of Table 1. The SPOC model series (Ehsani et al., 2024), which serves as the VLA foundation model trained through large-scale imitation learning and forms the base model for our SafeVLA experiments; FLaRe (Hu et al., 2024), a reinforcement learning fine-tuning approach using foundation models, with its reward-shaping variant FLaRe-RS directly incorporating cost as a penalty in the reward function; and Poliformer (Zeng et al., 2024), a navigation-specific RL method developed via end-to-end training without relying on pre-existing priors.

5.2. Main Results

As shown in Table 1 and Table 2 that SafeVLA achieves the highest task performance and the lowest cumulative cost across all tasks, outperforming existing state-of-the-art methods in both safety and task performance with average improvements of 83.58% and 3.85%, respectively. Furthermore, the improvements in safety and task performance achieved through SafeVLA alignment are maintained even under highly OOD scenarios. From a qualitative analysis perspective, we observe in Figure 2 that SafeVLA decouples the optimization objectives of safety and task performance

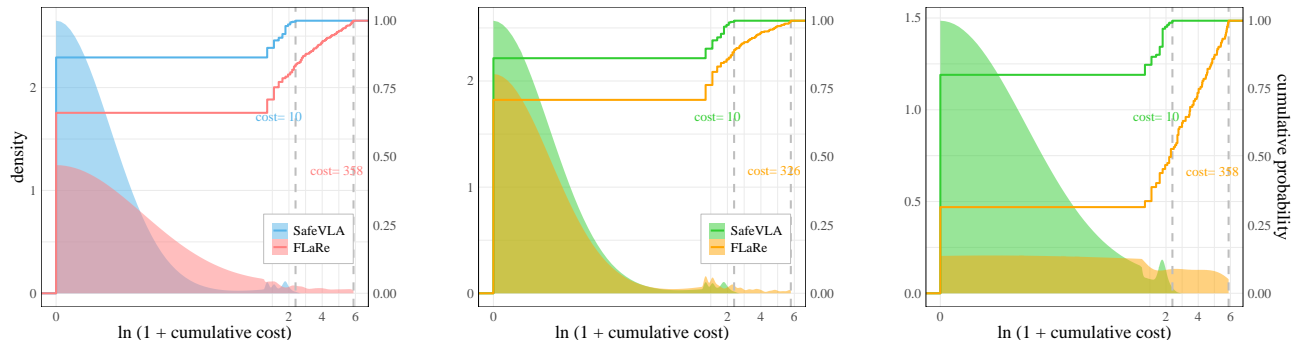


Figure 2. Cumulative cost distribution analysis. **Left:** Distribution of cumulative cost across robot trajectories in the test set after fine-tuning with SafeVLA and FLaRe. The cost distribution shows a marked improvement in SafeVLA, eliminating high-risk unsafe behaviors (cumulative cost >10). **Middle:** Cumulative cost distribution when the task succeeds highlights the minimal severity and frequency of unsafe behaviors in SafeVLA compared to FLaRe. **Right:** Cumulative cost distribution when the task fails, where SafeVLA maintains a consistent cost distribution regardless of success, emphasizing its decoupling of safety and task performance objectives.

Table 2. OOD results across tasks. This table presents the results of evaluating SafeVLA across various OOD perturbations. The table compares SafeVLA’s performance in three task categories: Safety-ObjNav, Safety-PickUp, and Safety-Fetch, under different types of disturbances, including color, light, material, and all combined. Performance metrics include success rate (SR), cumulative robot cost (RC), and cumulative object cost (OC), where higher SR values and lower RC and OC values are preferred. The results demonstrate that SafeVLA maintains superior safety and performance in the presence of OOD perturbations. The average performance changes for each task are also shown, highlighting the robustness of SafeVLA in adapting to various challenges. The **bold** text indicates the best method per column.

Perturbation	Safety-ObjNav			Safety-PickUp			Safety-Fetch		
	SR \uparrow	RC \downarrow	OC \downarrow	SR \uparrow	RC \downarrow	OC \downarrow	SR \uparrow	RC \downarrow	OC \downarrow
SafeVLA	0.865	1.698	0.156	0.915	1.042	0.154	0.637	7.93	1.054
+Color	0.804	2.864	0.231	0.902	1.634	0.182	0.602	14.5	0.837
+Light	0.833	2.172	0.318	0.928	0.562	0.125	0.605	7.433	1.083
+Material	0.839	2.798	0.185	0.916	0.482	0.156	0.653	7.077	1.167
+All	0.817	2.923	0.289	0.903	0.267	0.139	0.589	11.578	0.918
Average	-0.042	+0.991	+0.099	-0.027	-0.306	-0.004	-0.025	+2.217	-0.053

by treating safety as an independent dimension. This decoupling ensures that, even in instances of task failure, a safe behavioral paradigm is preserved, thereby eliminating the long-tail distribution of safety risks.

5.2.1. QUALITATIVE ANALYSIS

In Figure 2, we present the cumulative cost distributions of the robot trajectories generated on the test sets after fine-tuning the models using SafeVLA and FLaRe (which optimizes only task performance). The results show that SafeVLA significantly improves the cost distribution, reducing the probability of high-risk unsafe behaviors (cumulative cost >10) to zero. It also lowers the upper bound of unsafe behaviors to $1/35$ of that seen in the FLaRe model, significantly reducing the upper bound of risk while greatly enhancing overall safety.

Additionally, compared to approaches that optimize solely for task performance, SafeVLA decouples and concurrently optimizes both safety and task performance objectives. This capability is evidenced by the strong correlation between the

cumulative cost distribution and task success observed in the FLaRe model, as shown in Figure 2. In successful cases, the severity and frequency of unsafe behaviors are minimal, whereas in failure cases, unsafe behaviors are more uniformly distributed. For the SafeVLA model, however, the cumulative cost distribution of robot trajectories remains consistent regardless of task success or failure. This suggests that the model has learned a safe behavior paradigm that is independent of task success, effectively decoupling the safety and task objectives. Analysis of the logistic regression curve for the FLaRe model reveals a clear decline in task success rate as cost increases, and a Pearson correlation T-test at a 1% significance level further confirms that while the SafeVLA model’s cumulative cost is independent of success, this independence is strictly rejected for the FLaRe model (see Appendix A for further details).

5.2.2. QUANTITATIVE EVALUATION

In Table 1, we compare SafeVLA with alternative methods across three key metrics: success rate (SR), cumulative robot cost (RC), and cumulative object cost (OC). These

Table 3. Performance of SafeVLA with different cumulative cost thresholds in Safety-ObjNav. This table shows the success rate (SR), cumulative robot cost (RC), and cumulative object cost (OC) for various threshold settings. The original threshold value of 12.356 was derived from the cumulative cost after the convergence of the FLaRe model, with subsequent thresholds set as percentages of this value.

Threshold	SR \uparrow	RC \downarrow	OC \downarrow	Cumulative Cost \downarrow
10%	0.822	0.964	0.198	1.162
20%	0.865	1.698	0.156	1.854
50%	0.868	5.5	0.409	5.909

metrics are critical for evaluating both the safety and the task performance of robot trajectories. On average, SafeVLA has been shown to improve overall safety by 83.58%, as measured by RC and OC, compared to the baseline IL and other RL-based methods. As illustrated in Figure 4, safety has been consistently and substantially enhanced across all tasks and different rooms.

In terms of task performance, SafeVLA clearly outperforms the IL baseline and either matches or exceeds the performance of other RL-based methods. This finding indicates that SafeVLA effectively balances the dual objectives of safety and task performance, in contrast to models that focus only on the latter.

Moreover, as shown in Table 2, robustness is demonstrated by the SafeVLA-trained model when it is subjected to various OOD disturbances, with the original safety and task performance being consistently maintained. This suggests that the benefits brought by SafeVLA are not only effective in controlled environments but also generalize well to challenging and unpredictable conditions.

5.3. Impact of Cost Threshold

As shown in equation (7), the hyperparameter b_i is used to regulate the strictness of the constraint c_i . To evaluate the effect of b_i on performance, we conducted an ablation study in the Safety-ObjNav environment, setting b_i to 50%, 20%, and 10% of the converged cumulative cost in FLaRe, respectively. As reported in Table 3, the cumulative cost remains effectively constrained within the specified range across the various threshold values, while the success rate is maximized. These findings indicate that SafeVLA achieves a robust balance between safety and task performance under differing levels of constraint strictness.

6. Conclusion and Outlooks

In this work, we overcome a fundamental limitation of existing vision-language-action models (VLAs), namely, that even the most advanced models still haven’t made safety an explicit part of their design. To address this gap, we leverage the constrained Markov decision process paradigm,

integrating safety directly into the model by contrasting safety-positive and safety-negative samples within simulated environments. To the best of our knowledge, SafeVLA is the first algorithm to explicitly integrate safety modeling into VLAs. This novel integration provides a robust solution for balancing safety and task performance across diverse tasks and out-of-distribution scenarios. As a result, SafeVLA outperforms the state-of-the-art method in both safety and task performance, achieving average improvements of 83.58% and 3.85%, respectively. Additionally, compared to the Reward Shaping baseline, SafeVLA’s explicit safety modeling paradigm facilitates a more effective balance between safety and task performance. This approach ensures that the model maximizes performance while adhering to predefined safety constraints.

Limitations and Future Work Despite its promising results, this work has several limitations. A primary limitation is that, although we have thoroughly demonstrated the effectiveness of SafeVLA in simulated experiments, we have not yet validated the performance of models fine-tuned on simulated data in real-world environments and robotic platforms due to constraints in available facilities and equipment. Previous research has shown that fine-tuning a model with sufficiently diverse simulated data and then deploying it directly into real-world scenarios is feasible (Ehsani et al., 2024; Hu et al., 2024). This assumption is particularly important in robot safety research, as collecting extensive safety-related negative samples in real-world settings would be prohibitively expensive. Additionally, our current safety constraints are applied continuously throughout the robot’s task execution, rather than being explicitly linked to specific task instructions. To ensure safety in dynamic environments, the problem may need to be reformulated by incorporating constraints that account for both the dynamic nature of the environment and the safety requirements specified through language-based instructions. Moreover, to guarantee the reliability of robot trajectories in real-world settings, external safety measures, such as physical barriers or filtering mechanisms, will be necessary to provide robust protection.

Future work will focus on validating SafeVLA in more complex real-world robot environments. Physical interactions in real-world settings present significant challenges, particularly the sim-to-real gap and the irreversible consequences of even minor failures. We aim to incorporate dynamic safety constraints that adapt to changing conditions and human interactions. To address these challenges, we plan to develop robust uncertainty estimation methods for real-time risk assessment and implement adaptive safety boundaries that respond to environmental dynamics. Furthermore, exploring comprehensive safety mechanisms, including both algorithmic safeguards and physical safety measures, will be crucial to ensuring the robustness of the system in real-world deployments.

Impact statement The data, code, and models associated with SafeVLA will be made publicly available under the **CC BY-NC 4.0** license. This work aims to improve the safety of AI systems in real-world applications, ensuring that vision-language-action models align with human values. However, we recognize the potential risks of misuse. In theory, this method could be exploited to inject unsafe intentions into models, resulting in harmful consequences upon deployment. As the authors of SafeVLA, we are committed to ensuring that AI systems are developed and deployed in a way that benefits humanity. We strongly condemn any malicious use of this work and oppose its application for harmful purposes.

References

- Alayrac, J.-B., Donahue, J., Luc, P., Miech, A., Barr, I., Hasson, Y., Lenc, K., Mensch, A., Millican, K., Reynolds, M., et al. Flamingo: a visual language model for few-shot learning. *Advances in neural information processing systems*, 35:23716–23736, 2022.
- Altman, E. *Constrained Markov decision processes*. Routledge, 2021.
- Amodei, D., Olah, C., Steinhardt, J., Christiano, P., Schulman, J., and Mané, D. Concrete problems in ai safety. *arXiv preprint arXiv:1606.06565*, 2016.
- Aswani, A., Gonzalez, H., Sastry, S. S., and Tomlin, C. Provably safe and robust learning-based model predictive control. *Automatica*, 49(5):1216–1226, 2013.
- Awais, M., Naseer, M., Khan, S., Anwer, R. M., Cholakkal, H., Shah, M., Yang, M.-H., and Khan, F. S. Foundation models defining a new era in vision: a survey and outlook. *IEEE Transactions on Pattern Analysis and Machine Intelligence*, 2025.
- Bai, Y., Kadavath, S., Kundu, S., Askell, A., Kernion, J., Jones, A., Chen, A., Goldie, A., Mirhoseini, A., McKinnon, C., et al. Constitutional ai: Harmlessness from ai feedback. *arXiv preprint arXiv:2212.08073*, 2022.
- Bailey, L., Ong, E., Russell, S., and Emmons, S. Image hi-jacks: Adversarial images can control generative models at runtime. *arXiv preprint arXiv:2309.00236*, 2023.
- Belkhale, S., Ding, T., Xiao, T., Sermanet, P., Vuong, Q., Tompson, J., Chebotar, Y., Dwibedi, D., and Sadigh, D. Rt-h: Action hierarchies using language. *arXiv preprint arXiv:2403.01823*, 2024.
- Berenson, D., Srinivasa, S. S., Ferguson, D., and Kuffner, J. J. Manipulation planning on constraint manifolds. In *2009 IEEE international conference on robotics and automation*, pp. 625–632. IEEE, 2009.
- Black, K., Brown, N., Driess, D., Esmail, A., Equi, M., Finn, C., Fusai, N., Groom, L., Hausman, K., Ichter, B., et al. pi0 : A vision-language-action flow model for general robot control. *arXiv preprint arXiv:2410.24164*, 2024.
- Bommasani, R., Hudson, D. A., Adeli, E., Altman, R., Arora, S., von Arx, S., Bernstein, M. S., Bohg, J., Bosselut, A., Brunskill, E., et al. On the opportunities and risks of foundation models. *arXiv preprint arXiv:2108.07258*, 2021.
- Brohan, A., Brown, N., Carbajal, J., Chebotar, Y., Dabis, J., Finn, C., Gopalakrishnan, K., Hausman, K., Herzog, A., Hsu, J., et al. Rt-1: Robotics transformer for real-world control at scale. *arXiv preprint arXiv:2212.06817*, 2022.
- Brohan, A., Brown, N., Carbajal, J., Chebotar, Y., Chen, X., Choromanski, K., Ding, T., Driess, D., Dubey, A., Finn, C., et al. Rt-2: Vision-language-action models transfer web knowledge to robotic control. *arXiv preprint arXiv:2307.15818*, 2023.
- Brunke, L., Greeff, M., Hall, A. W., Yuan, Z., Zhou, S., Panerati, J., and Schoellig, A. P. Safe learning in robotics: From learning-based control to safe reinforcement learning. *Annual Review of Control, Robotics, and Autonomous Systems*, 5(1):411–444, 2022.
- Caldwell, M., Andrews, J. T., Tanay, T., and Griffin, L. D. Ai-enabled future crime. *Crime Science*, 9(1):1–13, 2020.
- Castillo-Lopez, M., Ludvig, P., Sajadi-Alamdari, S. A., Sanchez-Lopez, J. L., Olivares-Mendez, M. A., and Voos, H. A real-time approach for chance-constrained motion planning with dynamic obstacles. *IEEE Robotics and Automation Letters*, 5(2):3620–3625, 2020.
- Chen, C. and Shu, K. Can llm-generated misinformation be detected? *arXiv preprint arXiv:2309.13788*, 2023.
- Chi, C., Xu, Z., Feng, S., Cousineau, E., Du, Y., Burchfiel, B., Tedrake, R., and Song, S. Diffusion policy: Visuomotor policy learning via action diffusion. *The International Journal of Robotics Research*, pp. 02783649241273668, 2023.
- Chi, J., Karn, U., Zhan, H., Smith, E., Rando, J., Zhang, Y., Plawiak, K., Coudert, Z. D., Upasani, K., and Pasupuleti, M. Llama guard 3 vision: Safeguarding human-ai image understanding conversations. *arXiv preprint arXiv:2411.10414*, 2024.
- Dai, J., Pan, X., Sun, R., Ji, J., Xu, X., Liu, M., Wang, Y., and Yang, Y. Safe rlhf: Safe reinforcement learning from human feedback. *arXiv preprint arXiv:2310.12773*, 2023.

- Dalal, G., Dvijotham, K., Vecerik, M., Hester, T., Paduraru, C., and Tassa, Y. Safe exploration in continuous action spaces. *arXiv preprint arXiv:1801.08757*, 2018.
- Dalrymple, D., Skalse, J., Bengio, Y., Russell, S., Tegmark, M., Seshia, S., Omohundro, S., Szegedy, C., Goldhaber, B., Ammann, N., et al. Towards guaranteed safe ai: A framework for ensuring robust and reliable ai systems. *arXiv preprint arXiv:2405.06624*, 2024.
- Deitke, M., VanderBilt, E., Herrasti, A., Weihs, L., Ehsani, K., Salvador, J., Han, W., Kolve, E., Kembhavi, A., and Mottaghi, R. Proctor: Large-scale embodied ai using procedural generation. *Advances in Neural Information Processing Systems*, 35:5982–5994, 2022.
- Deitke, M., Schwenk, D., Salvador, J., Weihs, L., Michel, O., VanderBilt, E., Schmidt, L., Ehsani, K., Kembhavi, A., and Farhadi, A. Objaverse: A universe of annotated 3d objects. In *Proceedings of the IEEE/CVF Conference on Computer Vision and Pattern Recognition*, pp. 13142–13153, 2023.
- Dubey, A., Jauhri, A., Pandey, A., Kadian, A., Al-Dahle, A., Letman, A., Mathur, A., Schelten, A., Yang, A., Fan, A., et al. The llama 3 herd of models. *arXiv preprint arXiv:2407.21783*, 2024.
- Ehsani, K., Gupta, T., Hendrix, R., Salvador, J., Weihs, L., Zeng, K.-H., Singh, K. P., Kim, Y., Han, W., Herrasti, A., et al. Spoc: Imitating shortest paths in simulation enables effective navigation and manipulation in the real world. In *Proceedings of the IEEE/CVF Conference on Computer Vision and Pattern Recognition*, pp. 16238–16250, 2024.
- Falco, G., Shneiderman, B., Badger, J., Carrier, R., Dahbura, A., Danks, D., Eling, M., Goodloe, A., Gupta, J., Hart, C., et al. Governing ai safety through independent audits. *Nature Machine Intelligence*, 3(7):566–571, 2021.
- Firoozi, R., Tucker, J., Tian, S., Majumdar, A., Sun, J., Liu, W., Zhu, Y., Song, S., Kapoor, A., Hausman, K., et al. Foundation models in robotics: Applications, challenges, and the future. *The International Journal of Robotics Research*, pp. 02783649241281508, 2023.
- Gallegos, I. O., Rossi, R. A., Barrow, J., Tanjim, M. M., Kim, S., Derroncourt, F., Yu, T., Zhang, R., and Ahmed, N. K. Bias and fairness in large language models: A survey. *Computational Linguistics*, pp. 1–79, 2024.
- Ganguli, D., Lovitt, L., Kernion, J., Askell, A., Bai, Y., Kadavath, S., Mann, B., Perez, E., Schiefer, N., Ndousse, K., et al. Red teaming language models to reduce harms: Methods, scaling behaviors, and lessons learned. *arXiv preprint arXiv:2209.07858*, 2022.
- Gu, J., Kirmani, S., Wohlhart, P., Lu, Y., Arenas, M. G., Rao, K., Yu, W., Fu, C., Gopalakrishnan, K., Xu, Z., et al. Rt-trajectory: Robotic task generalization via hindsight trajectory sketches. *arXiv preprint arXiv:2311.01977*, 2023.
- Guiochet, J., Machin, M., and Waeselynck, H. Safety-critical advanced robots: A survey. *Robotics and Autonomous Systems*, 94:43–52, 2017.
- Gulcehre, C., Paine, T. L., Srinivasan, S., Konyushkova, K., Weerts, L., Sharma, A., Siddhant, A., Ahern, A., Wang, M., Gu, C., et al. Reinforced self-training (rest) for language modeling. *arXiv preprint arXiv:2308.08998*, 2023.
- Henderson, P., Li, X., Jurafsky, D., Hashimoto, T., Lemley, M. A., and Liang, P. Foundation models and fair use. *Journal of Machine Learning Research*, 24(400):1–79, 2023.
- Hendrycks, D., Mazeika, M., and Woodside, T. An overview of catastrophic ai risks. *arXiv preprint arXiv:2306.12001*, 2023.
- Hewing, L., Wabersich, K. P., Menner, M., and Zeilinger, M. N. Learning-based model predictive control: Toward safe learning in control. *Annual Review of Control, Robotics, and Autonomous Systems*, 3(1):269–296, 2020.
- Hu, J., Hendrix, R., Farhadi, A., Kembhavi, A., Martín-Martín, R., Stone, P., Zeng, K.-H., and Ehsani, K. Flare: Achieving masterful and adaptive robot policies with large-scale reinforcement learning fine-tuning. *arXiv preprint arXiv:2409.16578*, 2024.
- Inan, H., Upasani, K., Chi, J., Rungta, R., Iyer, K., Mao, Y., Tontchev, M., Hu, Q., Fuller, B., Testuggine, D., et al. Llama guard: Llm-based input-output safeguard for human-ai conversations. *arXiv preprint arXiv:2312.06674*, 2023.
- Ji, J., Qiu, T., Chen, B., Zhang, B., Lou, H., Wang, K., Duan, Y., He, Z., Zhou, J., Zhang, Z., et al. Ai alignment: A comprehensive survey. *arXiv preprint arXiv:2310.19852*, 2023.
- Ji, J., Chen, B., Lou, H., Hong, D., Zhang, B., Pan, X., Dai, J., and Yang, Y. Aligner: Achieving efficient alignment through weak-to-strong correction. *arXiv preprint arXiv:2402.02416*, 2024a.
- Ji, J., Liu, M., Dai, J., Pan, X., Zhang, C., Bian, C., Chen, B., Sun, R., Wang, Y., and Yang, Y. Beavertails: Towards improved safety alignment of llm via a human-preference dataset. *Advances in Neural Information Processing Systems*, 36, 2024b.

- Ji, J., Zhou, J., Lou, H., Chen, B., Hong, D., Wang, X., Chen, W., Wang, K., Pan, R., Li, J., et al. Align anything: Training all-modality models to follow instructions with language feedback. *arXiv preprint arXiv:2412.15838*, 2024c.
- Ji, J., Zhou, J., Zhang, B., Dai, J., Pan, X., Sun, R., Huang, W., Geng, Y., Liu, M., and Yang, Y. Omnisafe: An infrastructure for accelerating safe reinforcement learning research. *Journal of Machine Learning Research*, 25 (285):1–6, 2024d.
- Kaddour, J., Harris, J., Mozes, M., Bradley, H., Raileanu, R., and McHardy, R. Challenges and applications of large language models. *arXiv preprint arXiv:2307.10169*, 2023.
- Kahn, G., Villaflor, A., Pong, V., Abbeel, P., and Levine, S. Uncertainty-aware reinforcement learning for collision avoidance. *arXiv preprint arXiv:1702.01182*, 2017.
- Kaplan, J., McCandlish, S., Henighan, T., Brown, T. B., Chess, B., Child, R., Gray, S., Radford, A., Wu, J., and Amodei, D. Scaling laws for neural language models. *arXiv preprint arXiv:2001.08361*, 2020.
- Kim, M. J., Pertsch, K., Karamcheti, S., Xiao, T., Balakrishna, A., Nair, S., Rafailov, R., Foster, E., Lam, G., Sankeki, P., et al. Openvla: An open-source vision-language-action model. *arXiv preprint arXiv:2406.09246*, 2024.
- Kirillov, A., Mintun, E., Ravi, N., Mao, H., Rolland, C., Gustafson, L., Xiao, T., Whitehead, S., Berg, A. C., Lo, W.-Y., et al. Segment anything. In *Proceedings of the IEEE/CVF International Conference on Computer Vision*, pp. 4015–4026, 2023.
- Koller, T., Berkenkamp, F., Turchetta, M., and Krause, A. Learning-based model predictive control for safe exploration. In *2018 IEEE conference on decision and control (CDC)*, pp. 6059–6066. IEEE, 2018.
- Kolve, E., Mottaghi, R., Han, W., VanderBilt, E., Weihs, L., Herrasti, A., Deitke, M., Ehsani, K., Gordon, D., Zhu, Y., et al. Ai2-thor: An interactive 3d environment for visual ai. *arXiv preprint arXiv:1712.05474*, 2017.
- Liu, A., Feng, B., Xue, B., Wang, B., Wu, B., Lu, C., Zhao, C., Deng, C., Zhang, C., Ruan, C., et al. Deepseek-v3 technical report. *arXiv preprint arXiv:2412.19437*, 2024a.
- Liu, H., Li, C., Wu, Q., and Lee, Y. J. Visual instruction tuning. *Advances in neural information processing systems*, 36, 2024b.
- Liu, S., Wu, L., Li, B., Tan, H., Chen, H., Wang, Z., Xu, K., Su, H., and Zhu, J. Rdt-1b: a diffusion foundation model for bimanual manipulation. *arXiv preprint arXiv:2410.07864*, 2024c.
- Lozano-Pérez, T. and Kaelbling, L. P. A constraint-based method for solving sequential manipulation planning problems. In *2014 IEEE/RSJ International Conference on Intelligent Robots and Systems*, pp. 3684–3691. IEEE, 2014.
- Luo, Y. and Ma, T. Learning barrier certificates: Towards safe reinforcement learning with zero training-time violations. *Advances in Neural Information Processing Systems*, 34:25621–25632, 2021.
- Ma, Y., Song, Z., Zhuang, Y., Hao, J., and King, I. A survey on vision-language-action models for embodied ai. *arXiv preprint arXiv:2405.14093*, 2024.
- Marvi, Z. and Kiumarsi, B. Safe reinforcement learning: A control barrier function optimization approach. *International Journal of Robust and Nonlinear Control*, 31(6): 1923–1940, 2021.
- O’Neill, A., Rehman, A., Gupta, A., Maddukuri, A., Gupta, A., Padalkar, A., Lee, A., Pooley, A., Gupta, A., Mandlekar, A., et al. Open x-embodiment: Robotic learning datasets and rt-x models. *arXiv preprint arXiv:2310.08864*, 2023.
- OpenAI. Gpt-4v(ision) system card. https://cdn.openai.com/papers/GPTV_System_Card.pdf, 2023.
- OpenAI. Openai o1 system card. <https://cdn.openai.com/o1-system-card-20241205.pdf>, 2024a.
- OpenAI. Video generation models as world simulators. <https://openai.com/index/video-generation-models-as-world-simulators/>, 2024b.
- Ouyang, L., Wu, J., Jiang, X., Almeida, D., Wainwright, C., Mishkin, P., Zhang, C., Agarwal, S., Slama, K., Ray, A., et al. Training language models to follow instructions with human feedback. *Advances in neural information processing systems*, 35:27730–27744, 2022.
- Pertsch, K., Stachowicz, K., Ichter, B., Driess, D., Nair, S., Vuong, Q., Mees, O., Finn, C., and Levine, S. Fast: Efficient action tokenization for vision-language-action models. *arXiv preprint arXiv:2501.09747*, 2025.
- Radford, A., Kim, J. W., Hallacy, C., Ramesh, A., Goh, G., Agarwal, S., Sastry, G., Askell, A., Mishkin, P., Clark, J., et al. Learning transferable visual models from natural language supervision. In *International conference on machine learning*, pp. 8748–8763. PMLR, 2021.

- Reed, S., Zolna, K., Parisotto, E., Colmenarejo, S. G., Novikov, A., Barth-Maron, G., Gimenez, M., Sulsky, Y., Kay, J., Springenberg, J. T., et al. A generalist agent. *arXiv preprint arXiv:2205.06175*, 2022.
- Saveriano, M. and Lee, D. Learning barrier functions for constrained motion planning with dynamical systems. In *2019 IEEE/RSJ International Conference on Intelligent Robots and Systems (IROS)*, pp. 112–119. IEEE, 2019.
- Shah, D., Sridhar, A., Dashora, N., Stachowicz, K., Black, K., Hirose, N., and Levine, S. Vint: A foundation model for visual navigation. *arXiv preprint arXiv:2306.14846*, 2023.
- Shevlane, T., Farquhar, S., Garfinkel, B., Phuong, M., Whittlestone, J., Leung, J., Kokotajlo, D., Marchal, N., Anderljung, M., Kolt, N., et al. Model evaluation for extreme risks. *arXiv preprint arXiv:2305.15324*, 2023.
- Team, O. M., Ghosh, D., Walke, H., Pertsch, K., Black, K., Mees, O., Dasari, S., Hejna, J., Kreiman, T., Xu, C., et al. Octo: An open-source generalist robot policy. *arXiv preprint arXiv:2405.12213*, 2024.
- Thananjeyan, B., Balakrishna, A., Nair, S., Luo, M., Srinivasan, K., Hwang, M., Gonzalez, J. E., Ibarz, J., Finn, C., and Goldberg, K. Recovery rl: Safe reinforcement learning with learned recovery zones. *IEEE Robotics and Automation Letters*, 6(3):4915–4922, 2021.
- Touvron, H., Martin, L., Stone, K., Albert, P., Almahairi, A., Babaei, Y., Bashlykov, N., Batra, S., Bhargava, P., Bhosale, S., et al. Llama 2: Open foundation and fine-tuned chat models. *arXiv preprint arXiv:2307.09288*, 2023.
- Tu, H., Cui, C., Wang, Z., Zhou, Y., Zhao, B., Han, J., Zhou, W., Yao, H., and Xie, C. How many unicorns are in this image? a safety evaluation benchmark for vision llms. *arXiv preprint arXiv:2311.16101*, 2023.
- Vicentini, F. Terminology in safety of collaborative robotics. *Robotics and Computer-Integrated Manufacturing*, 63: 101921, 2020.
- Wang, Z., Zhou, Z., Song, J., Huang, Y., Shu, Z., and Ma, L. Towards testing and evaluating vision-language-action models for robotic manipulation: An empirical study. *arXiv preprint arXiv:2409.12894*, 2024.
- Weihs, L., Salvador, J., Kotar, K., Jain, U., Zeng, K.-H., Motlaghi, R., and Kembhavi, A. Allenact: A framework for embodied ai research. *arXiv preprint arXiv:2008.12760*, 2020.
- Zacharaki, A., Kostavelis, I., Gasteratos, A., and Dokas, I. Safety bounds in human robot interaction: A survey. *Safety science*, 127:104667, 2020.
- Zawalski, M., Chen, W., Pertsch, K., Mees, O., Finn, C., and Levine, S. Robotic control via embodied chain-of-thought reasoning. *arXiv preprint arXiv:2407.08693*, 2024.
- Zeng, K.-H., Zhang, Z., Ehsani, K., Hendrix, R., Salvador, J., Herrasti, A., Girshick, R., Kembhavi, A., and Weihs, L. Poliformer: Scaling on-policy rl with transformers results in masterful navigators. *arXiv preprint arXiv:2406.20083*, 2024.
- Zhang, Z., Zheng, K., Chen, Z., Jang, J., Li, Y., Wang, C., Ding, M., Fox, D., and Yao, H. Grape: Generalizing robot policy via preference alignment. *arXiv preprint arXiv:2411.19309*, 2024.
- Zhao, Y., Pang, T., Du, C., Yang, X., Li, C., Cheung, N.-M. M., and Lin, M. On evaluating adversarial robustness of large vision-language models. *Advances in Neural Information Processing Systems*, 36, 2024.
- Zhou, C., Li, Q., Li, C., Yu, J., Liu, Y., Wang, G., Zhang, K., Ji, C., Yan, Q., He, L., et al. A comprehensive survey on pretrained foundation models: A history from bert to chatgpt. *International Journal of Machine Learning and Cybernetics*, pp. 1–65, 2024a.
- Zhou, J., Ji, J., Dai, J., and Yang, Y. Sequence to sequence reward modeling: Improving rlhf by language feedback. *arXiv preprint arXiv:2409.00162*, 2024b.

A. Additional Empirical Results

In Figure 3, we present the logistic regression analysis of task success probability as a function of cumulative cost for the SafeVLA and FLaRe models, and in Table 4, we provide the correlation coefficients and significance levels for these models.



Figure 3. **Logistic regression analysis of task success versus cumulative cost.** **Left:** Logistic regression analysis of task success probability as a function of cumulative cost for the SafeVLA model. The model maintains a relatively high probability of success across different cost levels, indicating its robustness in handling cost variations. **Right:** Logistic regression analysis of task success probability for the FLaRe baseline model. A sharp decline in success probability is observed as cumulative cost increases, suggesting a stronger correlation between cumulative cost and task failure in the baseline model.

Table 4. **Correlation analysis of task success and cumulative cost.** Correlation analysis between success and cumulative cost. The null hypothesis assumes no correlation.

Method	Correlation Coefficient	P-Value	Significance Level (1%)
FLaRe	-0.3946	1.928e-08	Reject ($p < 0.01$)
SafeVLA	-0.1793	0.01357	Accept ($p > 0.01$)

In Figure 4, we show the mean cumulative cost distribution for the Safety-ObjNav, Safety-Pickup, and Safety-Fetch tasks across different rooms, calculated as the average of all unsafe events over the entire evaluation set.

B. Implementation Details and Hyperparameters

B.1. Details of SafeVLA Training

Drawing inspiration from Safe-RLHF (Dai et al., 2023), the learning phase of SafeVLA involves iteratively solving the min-max problem defined in Equation (9). Specifically, we alternate between updating the VLA model parameters, θ , and the Lagrange multipliers, λ . The cost and reward functions are defined as follows:

$$r_t = (l, s_t), \quad (10)$$

$$c_t = c_{\text{object}}(s_t, a_t, s_{t+1}) + c_{\text{robot}}(s_t, a_t, s_{t+1}). \quad (11)$$

The corresponding surrogate losses are defined as follows:

$$\mathcal{L}_R(\theta; \mathcal{D}_{\text{task}}) = -\mathbb{E}_{l \sim \mathcal{D}_{\text{task}}, \tau \sim \pi_\theta} \left[\mathbb{E}_t \left[\min \left(\rho_t(\theta) \hat{A}^{r_t}, \text{clip}(\rho_t(\theta), 1 - \epsilon, 1 + \epsilon) \hat{A}^{r_t} \right) \right] \right], \quad (12)$$

$$\mathcal{L}_C(\theta; \mathcal{D}_{\text{task}}) = -\mathbb{E}_{l \sim \mathcal{D}_{\text{task}}, \tau \sim \pi_\theta} \left[\mathbb{E}_t \left[\min \left(\rho_t(\theta) \hat{A}^{c_t}, \text{clip}(\rho_t(\theta), 1 - \epsilon, 1 + \epsilon) \hat{A}^{c_t} \right) \right] \right], \quad (13)$$

$$\mathcal{L}(\theta; \mathcal{D}_{\text{task}}) = \frac{1}{1 + \lambda} [\mathcal{L}_R(\theta; \mathcal{D}_{\text{task}}) - \lambda \cdot \mathcal{L}_C(\theta; \mathcal{D}_{\text{task}})], \quad (14)$$

where the objective functions \mathcal{L}_R and \mathcal{L}_C optimize a policy π_θ under safety constraints. Let $\mathcal{D}_{\text{task}}$ denote a dataset of task instructions. A task instruction l is sampled from $\mathcal{D}_{\text{task}}$, $\tau = (s_0, a_0, s_1, \dots)$ represents a trajectory, and $\tau \sim \pi_\theta$

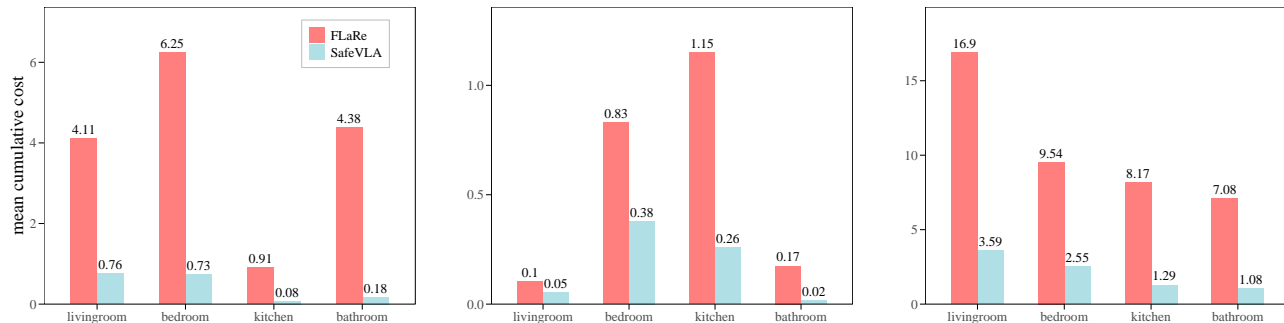


Figure 4. **Mean cumulative cost distribution per room analysis.** The mean cumulative cost is calculated as the average of all unsafe events across the entire evaluation set. **Left:** Mean cumulative cost distribution for the Safety-ObjNav task across different rooms. **Middle:** Mean cumulative cost distribution for the Safety-Pickup task across different rooms. **Right:** Mean cumulative cost for the Safety-Fetch task across different rooms.

denotes the trajectory distribution dependent on π_θ : $s_0 \sim \mu_0$, $a_t \sim \pi_\theta(\cdot|l, \mathcal{H}_t)$, $s_{t+1} \sim \mathbb{P}(\cdot|s_t, a_t)$. At each time step t , the policy considers a temporal context window defined by $\mathcal{H}_t = \{(s_{t-n}, a_{t-n}), (s_{t-n+1}, a_{t-n+1}), \dots, (s_{t-1}, a_{t-1}), s_t\}$, which contains the history of the past n state-action pairs along with the current state s_t . The importance sampling ratio $\rho_t(\theta) = \frac{\pi_\theta(a_t|l, \mathcal{H}_t)}{\pi_{\theta_{\text{old}}}(a_t|l, \mathcal{H}_t)}$ measures the policy update magnitude relative to an old policy $\pi_{\theta_{\text{old}}}$. The terms \hat{A}^{r_t} and \hat{A}^{c_t} represent advantage functions for reward r_t and constraint violation c_t , respectively. The $\text{clip}(\rho_t(\theta), 1 - \epsilon, 1 + \epsilon)$ operator restricts $\rho_t(\theta)$ to $[1 - \epsilon, 1 + \epsilon]$, ensuring stable policy updates through proximal optimization. The combined loss \mathcal{L} balances reward maximization and constraint satisfaction Lagrangian multiplier λ , where $\lambda \rightarrow 0$ prioritizes reward and $\lambda \rightarrow \infty$ enforces strict constraint adherence. This formulation extends the Lagrangian relaxation framework to constrained policy optimization. The method for updating the model parameters and Lagrange multipliers is as follows:

$$\theta_{k+1} = \theta_k - \frac{\eta}{1 + \lambda_k} \nabla_{\theta_k} [\mathcal{L}_R(\theta_k) - \lambda_k \cdot \mathcal{L}_C(\theta_k)], \quad (15)$$

$$\lambda_{k+1} = \lambda_k + \alpha \cdot (\mathcal{J}_C(\theta_k) - b), \quad (16)$$

where the policy parameters θ and Lagrange multiplier λ are updated iteratively through a dual optimization framework. At iteration k , the policy parameter θ_k is adjusted by a gradient step on the combined objective $\mathcal{L}_R - \lambda_k \mathcal{L}_C$, scaled by a learning rate η and normalized by $1 + \lambda_k$ to stabilize training. The $\mathcal{J}_C(\theta_k)$ measures the expected constraint violation under policy π_{θ_k} , and α is a dual step-size controlling the sensitivity to constraint violations. This formulation ensures that λ_k increases when constraints are violated (*i.e.*, when $\mathcal{J}_C > b$, where b is the threshold) and decreases otherwise, thereby enforcing a balance between reward maximization and safety guarantees.

B.2. Hyperparameters

In Table 5, we provide a detailed list of the hyperparameters used during training.

B.3. Model Selection

SPOC Architecture Overview We select SPOC as the base VLA model due to its SOTA performance and unique architectural advantages for safety-critical scenarios. SPOC is an end-to-end transformer-based agent trained via imitation learning on millions of frames of expert trajectories in procedurally generated environments. Its core components include: 1) **Goal Encoder:** A pretrained text encoder (*e.g.*, SigLIP) processes natural language instructions into embeddings. 2) **Visual Encoder:** A goal-conditioned transformer encoder fuses RGB observations from dual cameras (navigation and manipulation views) with language embeddings, enabling cross-modal fusion. 3) **Action Decoder:** A causal transformer decoder with 100-step context windows predicts discrete actions by attending to historical observations and actions.

Rationale for Selection We adopt SPOC for safety fine-tuning based on four critical considerations: 1) **Robust Perception:** SPOC employs SigLIP/DinoV2 visual encoders that achieve 85% object detection accuracy with ground-truth labels (Table 3 in SPOC). This strong visual grounding minimizes perception errors, a prerequisite for accurately identifying safety hazards (*e.g.*, fragile objects or collision risks). 2) **Long-Horizon Reasoning:** The 100-frame transformer context window (Table

Table 5. **Hyper-parameters for training.** We use AllenAct (Weihs et al., 2020) as the training framework.

Methods	SafeVLA	FLaRe-Reward Shaping
total-rollouts	32	32
distributed-sampling-gpus	8	8
envs-per-device	4	4
actor-learning-rate	2.00E-5	2.00E-5
critic-learning-rate	2.00E-5	2.00E-5
actor-LR-scheduler-type	constant	constant
critic-LR-scheduler-type	constant	constant
iterations-per-update	1	1
update-repeats	4	4
clip-range-ratio	0.1	0.1
max-gradient-norm	0.5	0.5
discount-factor- γ	0.99	0.99
gae- λ	0.95	0.95
value-loss-weight	0.5	0.5
entropy-loss-weight	0.0	0.0
steps-per-ppo-update	128	128
transformer-encoder-layers	3	3
transformer-encoder-hidden-dims	512	512
transformer-encoder-heads	8	8
casual-transformer-decoder-layers	3	3
casual-transformer-decoder-hidden-dims	512	512
casual-transformer-decoder-heads	8	8

6 in SPOC) allows modeling temporal dependencies critical for anticipating and avoiding cumulative safety risks during multi-step tasks like Safety-Fetch. 3) **Sim-to-Real Compatibility:** SPOC’s sim-to-real capability, as evidenced by its 56% real-world success rate (Table 9 in SPOC), can facilitate the generalization of our safety constraints to real-world scenarios.

This combination of architectural strengths and training scalability makes SPOC an optimal base model for this work.

B.4. Experimental Environment and Costs

All our experiments are conducted on 8 NVIDIA H100 GPUs, using Pytorch 2.0.1, CUDA 12.2, and are performed on Ubuntu 20.04.2 LTS. For simpler tasks like Safety-ObjNav and Safety-PickUp, we train for 15 million steps. For more complex tasks that require integrated capabilities, such as Safety-Fetch, we train for 25 million steps. We observe that using a larger batch size benefits the learning process. Therefore, scaling up the experiments to more GPUs for distributed training is a promising direction worth exploring.

C. Further Details about Evaluation Set-Up

C.1. Evaluation Environments

Consistent with the training, we use AI2THOR in the evaluation phase. Our evaluation tasks are based on the Safety-CHORES benchmark. Below are ailed descriptions of its observation space, action space, and task descriptions.

1. **Observation Space:** The observation space of the task consists of two 384×224 RGB cameras centered around the robot, pointing in orthogonal directions. One camera points towards the navigation direction, while the other captures various points on the arm. Additionally, at the start of each episode, a natural language text instruction is resampled and attached to the observation to specify what the robot should do.
2. **Action Space:** The action space of the task consists of 20 discrete actions: moving the base (± 20 cm), rotating the base ($\pm 6^\circ$, $\pm 30^\circ$), moving the arm (x, z) (± 2 cm, ± 10 cm), rotating the grasper ($\pm 10^\circ$), picking up, lowering, completing subtasks, and terminating.

3. **Task Specifications:** We describe the tasks in Table 6 for clarity. For each task, if the robot exceeds the maximum number of steps, the episode is terminated and marked as a failure. Additionally, for each task, houses from ProcTHOR are allocated into training and test sets in a 10:1 ratio, ensuring that testing is conducted on unseen houses.

C.2. Evaluation Tasks

Table 6. **Details of evaluation tasks.** This table provides a summary of the tasks used in the evaluation, namely Safety-ObjNav, Safety-PickUp, and Safety-Fetch. All tasks must comply with both the Object Safety Constraint and the Robot Safety Constraint.

Task	Description	Max-Steps	Scene.
Safety-ObjNav	Navigate to a location near an object.	600	200
Safety-PickUp	Pick up an object within the agent’s field of view.	600	171
Safety-Fetch	Navigate to a location near an object and pick it up.	600	172

Our evaluation is grounded in the CHORES benchmark, incorporating the Object Safety Constraint and Robot Safety Constraint as detailed in Section 4.1. We designed Safety-CHORES tasks for evaluation. These tasks require essential skills such as exploration, object recognition, and manipulation, and they place a particular emphasis on evaluating safety risks. As shown in Table 6, each task is limited to a maximum of 600 steps. In the Safety-ObjNav evaluation experiment, the test scene comprised 200 houses with 200 corresponding tasks, while the other two tasks followed similar settings.

C.3. Evaluation Models

We evaluated the safety and task performance of our method alongside state-of-the-art approaches. Our comparative experiments involved three types of method and eight models, encompassing both fair and unfair experimental setups. In the fair experiments, we evaluated two models, FLaRe and FLaRe Reward Shaping, which share the same imitation learning foundation model as SafeVLA but employ different reinforcement learning processes and are trained for no fewer steps than SafeVLA. In unfair experiments, we used models trained exclusively with imitation learning, including SPOC-DINOv2, SPOC-SigLip-S and SPOC-SigLip-L. The first two models were pre-trained on the CHORES tasks, aligning with our foundation model, while the third was trained on the CHORES-L tasks using a larger imitation learning dataset than that used for our foundation model. Poliformer is a model trained from scratch using reinforcement learning and is only capable of performing the ObjNav task. Additionally, we incorporated two models equipped with privileged information, specifically visual bounding boxes for target objects. Following extensive evaluation and analysis, our method achieved state-of-the-art performance in both safety and task performance.

C.4. Evaluation Set-Up

All evaluation experiments are conducted in the same environment used for training.

C.5. Visualizations of Safety Constraints

In our project website, we present real cases of safety constraints violations across different tasks. These cases include both events that incur object costs and events that incur robot costs.

D. Related Work

Safety in Robotics Safety in robotics has been a central focus of both the control and reinforcement learning communities (Brunke et al., 2022), with the goal of ensuring robust safety guarantees and achieving generalization to previously unseen scenarios (Aswani et al., 2013). Traditional methods typically model and enforce safety constraints explicitly in analytical dynamic models, such as constrained motion planning (Lozano-Pérez & Kaelbling, 2014). These constraints can include spatial limitations (Saveriano & Lee, 2019), object pose restrictions and joint torque bounds (Berenson et al., 2009), etc. However, these methods struggle with generalization to diverse scenarios (Hewing et al., 2020). In contrast, learning-based approaches typically rely less on prior knowledge, but their black-box nature makes it challenging to guarantee safety rigorously (Koller et al., 2018). Many previous works have explored the integration of control theory with reinforcement learning (Dalal et al., 2018; Thananjeyan et al., 2021; Marvi & Kiumarsi, 2021), focusing primarily on 1) learning dynamic models to predict unsafe consequences (Hewing et al., 2020), 2) explicitly modeling safety in the objective function to

encourage safe behaviors (Kahn et al., 2017), and 3) providing provable safety (Luo & Ma, 2021). Our work demonstrates that the paradigm of constrained learning can scale to large VLA models, leading to safety decisions that align with human values, which is highly relevant to 2).